Original Article

Metabolic stress-induced dysregulation of the Hippo signaling pathway inhibits the occurrence of hepatocarcinoma

Shengming Zhang^{1,2*}, Lixiang Li^{1,2,3*}, Lei Jin^{1,2*}, Ziyi Li^{1,2*}, Qianqian Tao^{1,2}, Fuhai Zhou^{1,2}, Xingyang Lu^{1,2}, Qi Zhang^{1,2}, Gaobin Hu^{1,2}, Long Huang^{1,2}, Liangliang Zhang⁴, Qiyu Feng⁵, Hui Peng^{1,2}, Qingsheng Yu^{1,2}

¹Department of General Surgery, The First Affiliated Hospital of Anhui University of Chinese Medicine, Hefei 230031, Anhui, P. R. China; ²Institute of Chinese Medicine Surgery, Anhui Academy of Chinese Medicine, Hefei 230031, Anhui, P. R. China; ³Department of General Surgery, The People's Hospital of Lujiang County, No. 32, Wenming Middle Road, Lujiang County, Hefei 230031, Anhui, P. R. China; ⁴Affiliated Hospital of The Institute of Neurology, Anhui University of Chinese Medicine, Hefei 230061, Anhui, P. R. China; ⁵Cancer Research Center, The First Affiliated Hospital of USTC, Division of Life Sciences and Medicine, University of Science and Technology of China, Hefei 230036, Anhui, P. R. China. *Equal contributors.

Received January 1, 2025; Accepted August 29, 2025; Epub September 15, 2025; Published September 30, 2025

Abstract: Liver fibrosis is the natural stress response of the liver to injury and a critical intermediate stage in the progression of most liver diseases. Here, we first demonstrated *via* a retrospective clinical study that the incidence of advanced hepatocellular carcinoma (HCC) was significantly higher in patients infected with hepatitis B virus (HBV) than in those with hepatolenticular degeneration (HLD). Further analyses involving micro RNA (miRNA) and proteomics were conducted to investigate the distinct mechanisms underlying liver fibrosis induced by HBV and HLD. Results showed significant changes in metabolic pathways and molecules, especially in AMP-activated protein kinase (AMPK) and Hippo signaling pathways, which play crucial roles in cellular glucose and lipid metabolism. Characteristic of HLD is a mutation/deletion in the ATPase Copper Transporting Beta (ATP7B) gene. Subsequent studies indicated that the knockdown or overexpression of ATP7B mutants activates the AMPK and Hippo signaling pathways, resulting in the inhibition of proliferation and transformation of HCC cells. AMPK phosphorylation indicates the presence of metabolic stress. Thus, this finding might partly explain why patients with HLD-related liver fibrosis are more likely to develop liver failure rather than HCC, providing new insights into the intricate mechanisms linking metabolic orchestration and tumor development.

Keywords: Metabolic stress, liver fibrosis, hepatocellular carcinoma, Hippo, AMPK

Introduction

Liver damage, caused by viral hepatitis infection, alcohol abuse, autoimmune hepatitis, or metabolic disorders, triggers an inflammatory response that culminates in cell death and destruction within the liver [1, 2]. In response to liver injury, the body initiates a fibrotic process, producing collagen and protein to repair the damaged areas [3, 4]. This process, known as liver fibrosis, refers to the intermediate pathological state of connective tissue proliferation and is closely associated with subsequent liver diseases such as hepatocellular carcinoma and liver failure. Cirrhosis is the advanced

stage of liver fibrosis and has a high global incidence and mortality rate worldwide [5]. The World Health Organization estimates that over 2 million people worldwide are diagnosed with cirrhosis annually, resulting in more than 500,000 deaths [6]. The progression from cirrhosis to liver cancer or liver failure is poorly understood and the underlying mechanisms remain unclear.

As fibrosis is an intermediate stage in many liver diseases, the study of its molecular mechanisms is of particular importance [7, 8]. The Transforming Growth Factor-Beta (TGF- β)/ Smads signaling pathway is recognized as a piv-

otal mechanism involved in fibrosis. Following hepatocyte injury, the release of TGF-β triggers the activation of hepatic stellate cells, leading to the substantial production of collagen and driving the progression of liver fibrosis [9]. Furthermore, the involvement of additional signaling pathways such as platelet-derived growth factor (PDGF), Hedgehog (Hh), and the Wnt/B-catenin pathway is also significant in contributing to liver fibrosis [10, 11]. The liver is the largest metabolic organ in the body, and metabolic abnormalities appear to be a primary cause of several liver diseases. Therefore, a large number of studies have focused on the effects of abnormal metabolism on liver fibrosis and its subsequent processes. For instance, recent research has demonstrated that the Slc25a47 locus exerts influence over the metabolic regulation of liver fibrosis progression through its involvement in mitochondrial function [12], and that Bmal1 regulates hepatic stellate cell transformation in hepatic fibrosis via IDH1/α-KG-mediated glycolysis [13]. Given the close association between metabolic irregularities and the development as well as progression of liver disease, it is widely believed that these abnormalities play a pivotal role in the initiation of liver fibrosis and its subsequent progression to hepatocellular carcinoma [14-16].

Hepatitis B virus (HBV) infection is the most common cause of liver fibrosis [17-19], and such liver fibrosis is more likely to develop into hepatocellular carcinoma. Approximately 50% of liver cancer cases worldwide are attributed to HBV-induced liver fibrosis [20, 21]. In addition, patients with HBV-associated liver fibrosis have a significantly higher risk of developing hepatocarcinoma than those with liver fibrosis caused by other factors, and people infected with HBV have a more than 20-fold higher risk of hepatocarcinoma than uninfected individuals [22, 23]. Hepatocellular degenerative disease (HLD) is another factor leading to liver fibrosis, characterized by abnormal cellular metabolism due to mutations/deletion of ATPase Copper Transporting Beta (ATP7B) gene, which affects mitochondrial copper transport [24-26]. Advanced stages of HLD usually progress through liver fibrosis to cirrhosis rather than hepatocellular carcinoma [27], a phenomenon that has been noted in our clinical observations of more than 2,000 cases over the past three decades.

Both HBV infection and HLD can lead to metabolic abnormalities and inflammatory responsesin the liver [28, 29]. Statistics from over 300 clinical cases have shown that HLD-induced liver fibrosis is less likely to progress to hepatocarcinoma than HBV-induced fibrosis is. Therefore, this study aims to investigate the different molecular expressions and metabolic statuses associated with HBV infection and HLD-induced liver fibrosis. By investigating these differences, we hope to elucidate the underlying factors that contribute to the different outcomes in liver fibrosis and cirrhosis [30].

We compared the incidence of liver cancer between two groups of patients: those with HBV infection and those with HLD-related liver fibrosis. The results revealed a significantly higher incidence of advanced liver cancer in HBV-infected patients compared to the HLD group (HLD: 0.52%; HBV: 9.4%). To further investigate the molecular differences between two groups, we conducted miRNA and proteomic analysis on their liver tissues. Our analysis revealed significant differences in pathways and molecules, which were confirmed by subsequent proteomic and miRNA omics analysis. Of particular interest were the AMP-activated protein kinase (AMPK) and Hippo signaling pathways, known for their critical role in cellular glucose and lipid metabolism [31-33]. Further studies have shown that knockdown of ATP7B or overexpression of ATP7B mutants leads to AMPK phosphorylation and activation of the Hippo signaling pathway, which inhibits the proliferation and transformation of HCC cells in this particular condition [34]. This finding may partially explain why patients with HLD-related liver fibrosis are more likely to develop liver failure rather than liver cancer, and provides a new insights for further investigation into the intricate mechanisms linking metabolic orchestration and tumor development.

Materials and methods

Patient recruitment and clinical study

Clinical observations were initiated from April 2018 to November 2022 at the Department of General Surgery, The First Affiliated Hospital of Anhui University of Chinese Medicine, Anhui, China. All subjects gave their informed consent to participate before the start of the study. The demographics and clinical characteristics of the patients are shown in **Table 1**.

Table 1. The demographics and clinical characteristics of individuals

Baseline characteristics	HLD (n=191)	HBV (n=117)	P value
Female/Male	79/112	47/70	0.403
Mean age	26.58±10.76	56.25±11.36	< 0.05
BMI	16.23±2.59	19.03±3.56	< 0.05
Disease Cycle	15.76e .56	16.15e .56	0.421
ALT	74.20±19.62	36.29±12.67	< 0.05
AST	63.75±14.99	49.19±13.83	< 0.05
TBIL	38.73±11.56	34.67±18.02	0.593
TBA	45.73±15.32	39.41±11.42	0.377

HLD, Hepatolenticular degeneration; HBV, Hepatitis B virus; BMI, Body Mass Index; ALT, Alanine aminotransferase; AST, Aspartate aminotransferase; TBIL, Total bilirubin; TBA, Total bile acid.

Most patients were diagnosed with HLD or HBV. Patients suffering from other complications such as diarrhea were excluded. Blood biopsy were taken from the patients and blood profiles were determined, including Aspartate aminotransferase (AST), Alanine aminotransferase (ALT), total bilirubin (TBIL) and total bile acid (TBA). HLD and HBV tissue and adjacent healthy liver tissue were collected by splenectomy. All subjects agreed to publish their CT images. All clinical trial protocols were approved by the Ethics Committee of The First Affiliated Hospital of Anhui University of Chinese Medicine, Anhui, China (approval no. 2025-SYSFYSY-06).

Reagents

All ATP7B mutant lentiviruses were provided by OBiO Bio-technology Co. Ltd. (Shanghai, China). Compound C (HY-13418A) and verteporfin (HY-B0146) were purchased from the MCE MedChemExpress (Shanghai, China). Antibodies against caspase-3 (9662), FGF2 (61977) and enolase-2 (29528) were purchased from Cell Signaling Technology (Danvers, MA). APOB (ab20737), MRPS7 (ab224442) and MRPL3 (ab151326) antibodies were purchased from Abcam Ltd. (Cambridge, UK). Phospho-AMPK (P-AMPK) (50081s) and AMPK (5831s) antibodies were purchased from Cell Signaling Technology (Danvers, MA). Phospho-YAP (P-YAP) (13008), YAP (14074), phospho-TAZ (P-TAZ) (59971) and TAZ (72804) antibodies were purchased from Cell Signaling Technology (Danvers, MA). GADPH (60004-1) and β -actin (66009-1) antibodies were purchased from Proteintech Group (Rosement, IL, USA). Steriflip PVDF filters (0.1 or 0.22 µm pore size) and centrifugal filters were purchased from Millipore. Various primers for RT-PCR were purchased from RiboBio (Guangzhou, China).

Proteomics

SDT buffer was added to the sample, and transferred to 2 ml tubes with amount quartz sand. The lysate was homogenized by MP Fastprep-24 Automated Homogenizer (6.0 M/S, 30 s, twice). The homogenate was sonicated and then boiled for 15 min. After centrifuged at 14000 g for 40 min, the supernatant was filtered with 0.22 µm filters. The fil-

trate was quantified with the BCA Protein Assay Kit (P0012, Beyotime Biotechnology, China). The sample was stored at -20°C. Two hundred micrograms of proteins were reduced with 1 mM dithiotreitol and alkylated with 5.5 mM iodoacetamide. Proteins were digested with trypsin overnight, and stopped by 10% trifluoracetic acid. The peptides were desalted using C18 sep-pak cartridges and eluted with 1 ml methanol. Peptides were redissolved in Tetraethylammonium Bromide and labeled using TMT sixplex labeling reagent. The TMT-labeled peptides were combined and desalted by C18 sep-pak cartridges. The fractions were centrifuged and analyzed by LC-MS/MS. The TMTlabeled peptides were separated by gradient elution in a Thermo-Dionex Ultimate 3000 HPLC system. The analytical column was a home-made C18 resin packed fused silica capillary column. The Q Exactive mass spectrometer was operated by Xcalibur 2.1.2 software and 10 data-dependent MS/MS scans followed a single full-scan mass spectrum in the orbitrap. The peak lists from LC-MS/MS analysis were generated with Proteome Discoverer software. The MS/MS spectra were searched by the human FASTA database. Peptide spectral matches were validated using the Percolator at a 1% false discovery rate. The false discovery rate was set to 0.01 for protein identifications. Relative protein quantification was performed by Proteome Discoverer software. Protein ratios were calculated as the median of all peptide hits belonging to a protein. Quantitative precision was expressed as protein ratio variability. The biological meaning of proteomic data is first analyzed by Gene Ontology analysis and KEGG pathway enrichment. And we using SIGNOR database to generate a literature-based signaling information. The knowledge-based data obtained from STRING10 database is used to analyze the association within common, differently expressed proteins. Cytoscape 3.4.0 was used to visualize the common, differently expressed proteins.

High-throughput RNA-seq analysis

High-throughput RNA-seq analysis of tissues was performed at Genergy Co. Ltd. Total RNA was isolated by Trizol (Invitrogen, USA). The quantity and integrity of RNA yield was assessed by the Qubit® 2.0 (Life Technologies, USA) and Agilent 2200 TapeStation (Agilent Technologies, USA), respectively. For each sample, 1 µg of total RNA was used to prepare small RNA libraries using the NEBNext® Multiplex Small RNA Library Prep Set for Illumina (NEB, USA) according to the manufacturer's instructions. The libraries were sequenced by HiSeq 2500 (Illumina, USA) with single-end 50 bp at Genergy Co. Ltd. (Genergy, China).

Cell culture and transfections

The HCC cells (MHCC-97H and Huh-7) were confirmed to be free from mycoplasma contamination and were cultured in DMEM medium (C11965118BT, Gibco, USA) containing 10% FBS (Gibco, Australia), in an incubator of 5% $\rm CO_2$ at 37°C. The medium was replaced every 3 days. The cells were passaged by trypsinization when reaching ~80% confluency. Cells were seeded in individual plates. Following the manufacturer's instructions, expression constructs were transfected into cells with Polybrene (OBiO). After transfection, cells were washed twice with 1× PBS and the medium was replaced with complete medium 4-6 h after transfection.

Real-time quantitative PCR

Total RNA was extracted from cells with TRIzol reagent (Invitrogen, USA), as recommended by the manufacturer. Nanodrop (Thermo, USA) was used to quantify the concentration of RNA. cDNA was produced from 1 µg of total RNA using PrimeScript RT reagent KIT with gDNA Eraser (Perfect Real Time) (RRO47A; Takara). qRT-PCR was performed in triplicate with the

HiScript® II Q RT SuperMix for qPCR (+g DNA wiper) (R223, Vazyme Biotech, Nanjing, China) and the Roche LightCycler 96 System (Roche, Basel, Switzerland). The sequences were obtained from the GenBank nucleic acid sequence database (National Center for Biotechnology Information). Relative expression was calculated according to the 2-ΔΔCT method. U6 was used as the internal reference genes.

Western blot

Human or cell tissue was lysed with RIPA lysis buffer (Beyotime Biotechnology, China) according to the manufacturer's protocol. Protein concentrations were determined using the BCA protein assay kit (Beyotime Biotechnology, China). Proteins (20 µg) were separated via 10% SDS-PAGE, and subsequently transferred onto NC membranes (EMD Millipore). After transferred to a NC membrane, following blocking with 5% bovine plasma albumin, the membranes were washed three times with PBS. Subsequently, the membranes were incubated with primary antibodies at 4°C overnight. After washing with PBS, the membranes were incubated with H&L secondary antibody for 1 h at 25°C. Protein bands were visualized using the ECL Substrate kit (Thermofisher). Finally, Protein expression levels were semi-quantified using Image-Pro Plus software (version 6.0; Media Cybernetics, Inc.).

Periodic Acid Schiff stain (PAS)

The tissue slices from HLD and HBV patients was fixed a in PAS fixative solution and then stained with PAS for subsequent examination under a light microscope (Olympus, Tokyo, Japan). The PAS yielded signal was captured in full color using bright field. Images were converted to greyscale and the mean optical density of the PAS-derived signal was semi quantified per cell. More than 100 cells were scored per experiment. An image of PAS-staining without glycogen was captured to correct background optical density.

Cell proliferation assay

Cell proliferation assays were performed using the Cell Counting Kit-8 (CCK-8; Beyotime Biotechnology, Shanghai, China) according to the manufacturer's instructions. Briefly, cells were seeded onto 96-well plates (3 × 10³ cells per well) and treated with inhibitors when they reached 70-80%, and were then added with 10 μ L of CCK-8 solution, culturing for 1 h at 37°C in air with 5% CO $_2$ on designated days. The absorbance was measured at 450 nm using SynergyH1 (Biotek, Agilent, California, USA). For EdU assay, the cells were treated for 48 h, followed by using the BeyoClickTM EdU Cell Proliferation Kit with Alexa Fluor 594 (Beyotime Biotechnology, C0078S), according to the manufacturer's protocol.

Clonogenic assay

The hepatoma cell lines MHCC-97H and Huh-7 were either seeded into a 6-well plate (800-2500 cells per well) with or without agarose. The cells were cultured for 1-2 weeks in the presence of Compound C or verteporfin. For agarose-free culture, the cells were fixed with 4% paraformaldehyde and stained with crystal violet for 20 min. After washing with PBS, the number of colonies was counted. For agarose-containing culture, the number of clone clusters formed within the field of view under an inverted microscope was observed and quantified. Photographs were taken for both groups.

Data analyses

All results are presented as mean \pm SD. P values were calculated using Student's t-test for the comparison of differences between two groups. Significance among multiple groups was tested using one-way or two-way ANOVA. P < 0.05 was considered statistically significant.

Results

HLD patients exhibit a lower incidence of liver cancer

Liver fibrosis is an important nexus of liver lesions caused by a variety of factors. Our previous clinical observations have shown that fibrosis induced by HLD is less likely to lead to liver cancer than fibrosis induced by the hepatitis B virus (HBV). Based on this, we have presented cartoon diagrams and pathological slides of different stages in Figure 1A. There was no difference in blood fibrosis indices (data not shown) and imaging between HBV and HLD in the liver fibrotic stage; however, HBV-induced liver fibrosis is prone to develop into hepatocarcinoma (Figure 1B). Based on the above obser-

vations, data from more than 300 patients were collected from the First Affiliated Hospital of Anhui University of Chinese Medicine in 2019-2023, including HLD (191 cases) and HBV (117 cases), a total of 308 patients exhibited significant difference in physiological and pathological indicators including age, BMI, ALT, AST during liver fibrosis. Subsequent follow-up studies showed a significantly lower incidence of cancer in HLD patients compared to HBV patients (HLD: 0.52%; HBV: 11.97%), especially regarding hepatocellular carcinoma (HLD: 0.52%; HBV: 9.4%) (P < 0.05; Table 2). Statistically, HBV patients accounted for 50% to 80% of HCC cases worldwide [35], which is consistent with our clinical observations. The differential clinical data partially explains the reasons for the difference in tumor incidence between the HLD and HBV groups. However, the study observed that there was no significant difference in the course of the disease and pathological signs between the two groups, indicating that there must be other underlying mechanisms causing the disparity in tumor incidence between the two groups. Liver tissues from patients with hepatic hemangioma, HLD and HBV were collected during surgery (Figure S1A-I), Masson's staining showed normal liver tissues in patients with hepatic hemangioma (Figure S1B, S1C), while fibrous tissues in HLD and HBV patients were extensively proliferated, hepatic lobe space was enlarged, hepatocyte edema with a large number of inflammatory cell infiltration (Figure S1E, S1F, S1H, S1I). The above results indicate that despite the presence of fibrotic changes in liver tissue among HLD and HBV patients, the progression of liver fibrosis in these groups differs. Moreover, the incidence of liver cancer in HLD patients was significantly lower than that in HBV patients. In conclusion, according to the clinical statistics, CT reports, pathological specimens and multiple studies we collected, it was confirmed that HBV-induced liver fibrosis tends to develop into hepatocarcinoma, while HLD-induced liver fibrosis inhibits the occurrence of hepatocarcinoma and tends to liver failure, which is significantly different.

Proteomic differences between HLD and NOR patients

To further investigate the differential changes in liver fibrosis between patients with HLD or

Α HLD and HBV lead to different post-liver fibrosis progression HLD **HBV HCV ALD** Liver with cirrhosis HLD **NAFLD** Healthy liver Fibrotic liver **HBV** Liver cancer В CT Imaging of post-liver fibrosis progression of HLD and HBV Liver with cirrhosis HD Liver cancer 超

Figure 1. Patients with HLD have a low incidence of liver cancer. A. Schematic representation of liver fibrosis due to different etiologies leading to different outcomes. B. Imaging data of different outcomes of liver fibrosis caused by HLD (eventually leading to cirrhosis) and HBV (eventually leading to HCC).

NOR, we conducted proteomic and transcriptomic analyses on fresh tissue samples. Based on the proteomic analysis of 3 cases of HLD-induced cirrhosis and 3 cases of normal liver, we identified 305 significantly differentially expressed proteins between the two groups (top 15 in Heat map is shown in Figure 2A and top 15 in Volcano plot is shown in Figure 2B). Specifically, there were 219 proteins upregulated and 86 proteins downregulated in HLD patients compared to NOR patients (Figure 2C). Subsequent Gene Ontology (GO) analysis highlighted significant differences in biological processes, molecular function and cellular compo-

nent between the two groups, with a particular focus on abnormal metabolism (Figures 2D and S2A). KEGG pathway analysis revealed that the enriched pathways associated with the differentially expressed proteins were predominantly related to metabolism. These findings suggest the presence of distinct metabolic differences in the liver between the two groups of patients, which could potentially contribute to the observed divergent clinical outcomes observed (Figurse 2E and S2B). The results from protein-protein interaction network (PPI) analysis indicated a significant coordinated interaction between metabolic pathways in the

Table 2. Incidence of cancers

Cancer types	HLD (n=191)	HBV (n=117)	P value
Lung	0	1	0.201
Stomach	0	2	0.070
Liver	1	11	< 0.001
Pancreas	0	0	
Total	1	14	< 0.001

two groups (**Figure 2F**). The consistent results of protein quality control across different patient groups confirm the reliability of our analysis and hence the robustness of the results (<u>Figure S2C-H</u>).

Differentially expressed miRNAs between HLD and NOR patients

To compare the differences in miRNAs between patients with HLD-induced cirrhosis and normal tissues, RNA from liver tissue samples from both groups underwent sequencing. The RNA quality control of the isolated tissues from each patient group met the standard and is suitable for subsequent analysis (Figure S2A and S2B). The expression profiles of miRNAs between the two groups revealed that 21 miR-NAs were differentially expressed (The transcriptional data quality control can be seen in Figure S3A and S3B. Heat map was shown in Figure 3A and Volcano plot was shown in Figure 3B). Among them, 18 miRNAs were up-regulated and 3 miRNAs were down-regulated in the liver tissue of HLD patients compared to NOR patients (Figures 3C and S3C). GO functional analysis of the differentially expressed miRNAs showed that the differences between the two groups were observed in the Biological Process category, indicating their involvement in the regulation of biological functions (Figures 3D, S3D and S3E). KEGG pathway enrichment analysis revealed that the differences between the two groups were mainly associated with cancer development. This finding may provide insight into why patients with HLD-induced cirrhosis and HBV-induced cirrhosis exhibit different outcomes. Moreover, significant differences were observed in the Hippo and AMPK pathways between the two groups (Figure 3E). Network of miRNAs analysis revealed that the AMPK and Hippo signaling pathways interact with numerous cancer-related pathways (Figure 3F). The expression results of key miRNAs in tissues detected by qRT-PCR technology were consistent with the results of omics analysis (Figure 3G). Through these experiments, we have identified differences in key metabolic pathways, specifically the AMPK and Hippo signaling pathways, between the two patient groups, which interact with pathways involved in cancer development.

Transcriptomic analysis of mRNA and its integration with miRNA transcriptomics and proteomic analysis

Omics analysis of mRNAs in two groups of patients with HLD-induced cirrhosis or normal liver tissues revealed a large number of differentially expressed mRNAs between the two groups (Heat map is shown in Figure 4A and Volcano plot is shown in Figure 4B). GO functional analysis revealed that the differentially expressed mRNAs between the two groups were mainly enriched in stress response, which may be caused by liver cell damage in liver cirrhosis (Figure 4C). KEGG enrichment analysis identified enrichment in the AMPK signaling pathway and other pathways related to carbohydrate and glycolipid metabolism (Figure 4D), which is consistent with our findings in miRNA omics analysis. Previous studies have demonstrated the close association between glycolipid metabolism and the Hippo signaling pathway [36-38]. The combined analysis of miRNA and mRNA omics suggests the presence of 12 upregulated miRNAs and 3 downregulated miR-NAs that target the differentially expressed mRNAs. These changes in miRNAs resulted in the upregulation of 29 mRNAs and the downregulation of 22 mRNAs (Figure 4E), which is in line with our findings in the miRNA omics analysis. The intersection analysis of mRNA and protein omics results revealed an overlap of 131 mRNAs and proteins that were upregulated and 12 that were downregulated in both datasets, confirming the consistency between mRNA and protein omics results (Figure S4A-D). Combining these results with the differential expression of upstream miRNAs, we identified two consistently altered upstream miRNAs were found to target 5 downstream mRNAs and proteins (Figure 4F). Western blot (WB) results validated the expression of key proteins in the differentially regulated pathways identified by the omics analysis (Figure 4G). The results of the mRNA omics analysis further supported the consistent regulation of metabolic signaling pathways observed in the miRNA omics and protein

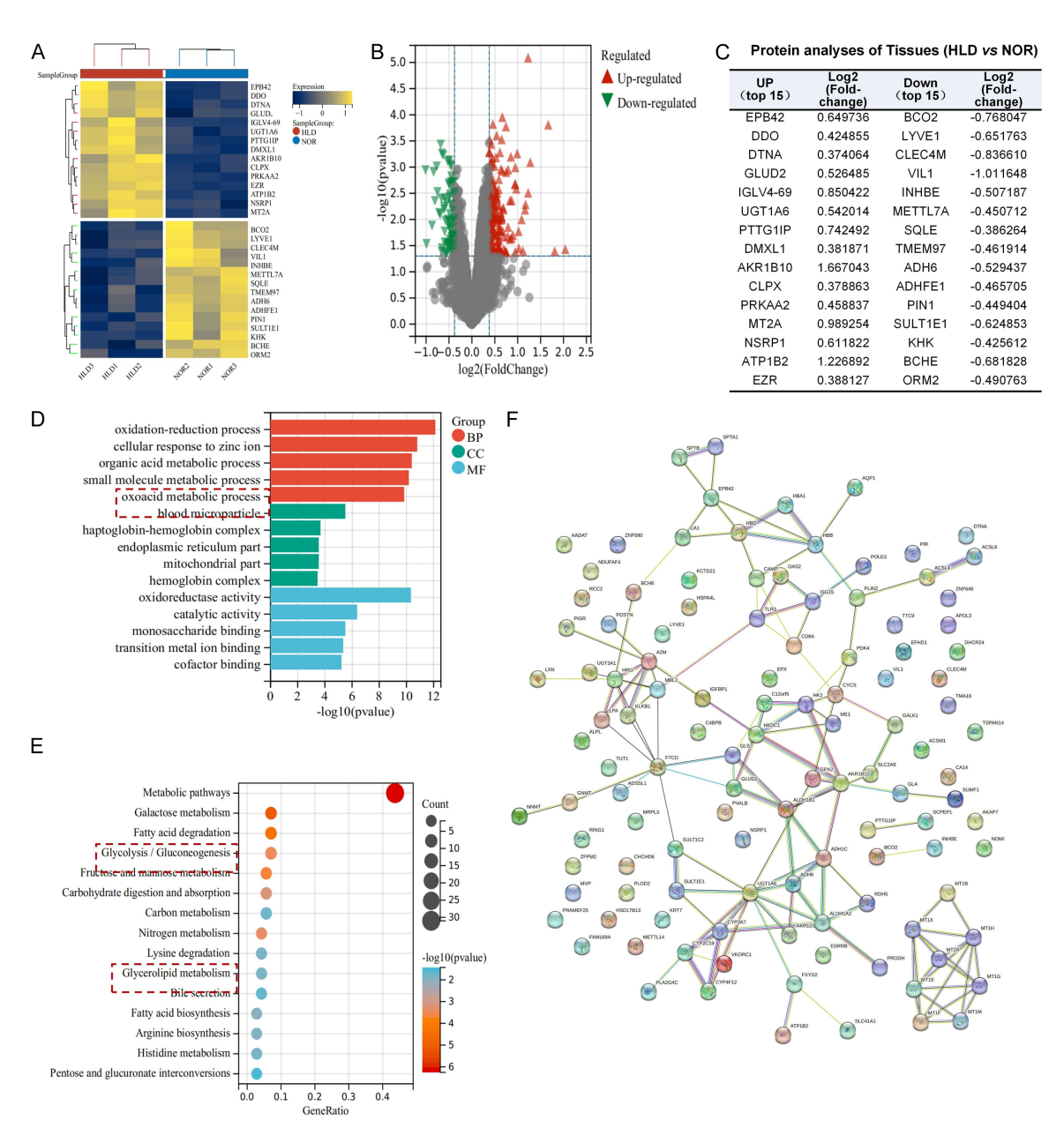


Figure 2. The profiling of proteins. A. Heat map of top 15 differentially expressed proteins in HLD and NOR. B. Volcano plot of differentially expressed proteins in HLD and NOR. C. List of proteins with increased and decreased expression in tissues of HLD and NOR patients. D. Gene Ontology (GO) term analysis. E. Target pathways of top 15 differential expressed proteins. F. Network of Protein-Protein Interaction (PPI) between NOR group and HLD group. HBV represents the Hepatitis B virus infection group, while HLD refers to hepatolenticular degeneration.

omics results, suggesting that these changes may be related to the stress response function.

The Hippo and AMPK pathways are activated in liver samples from HLD patients

The above omics analysis revealed that the protein and miRNA differences between HLD and

HBV were mainly enriched in glycolipid metabolism, and the Hippo and AMPK signaling pathways, and the Hippo signaling pathway is closely associated with tumor progression [39-41]. It was found that the AMPK and Hippo signaling pathways were activated in the liver tissues of HLD patients compared to the control group (*P < 0.05; Figure 5A), which was consistent with the omics results. Periodic Acid Schiff

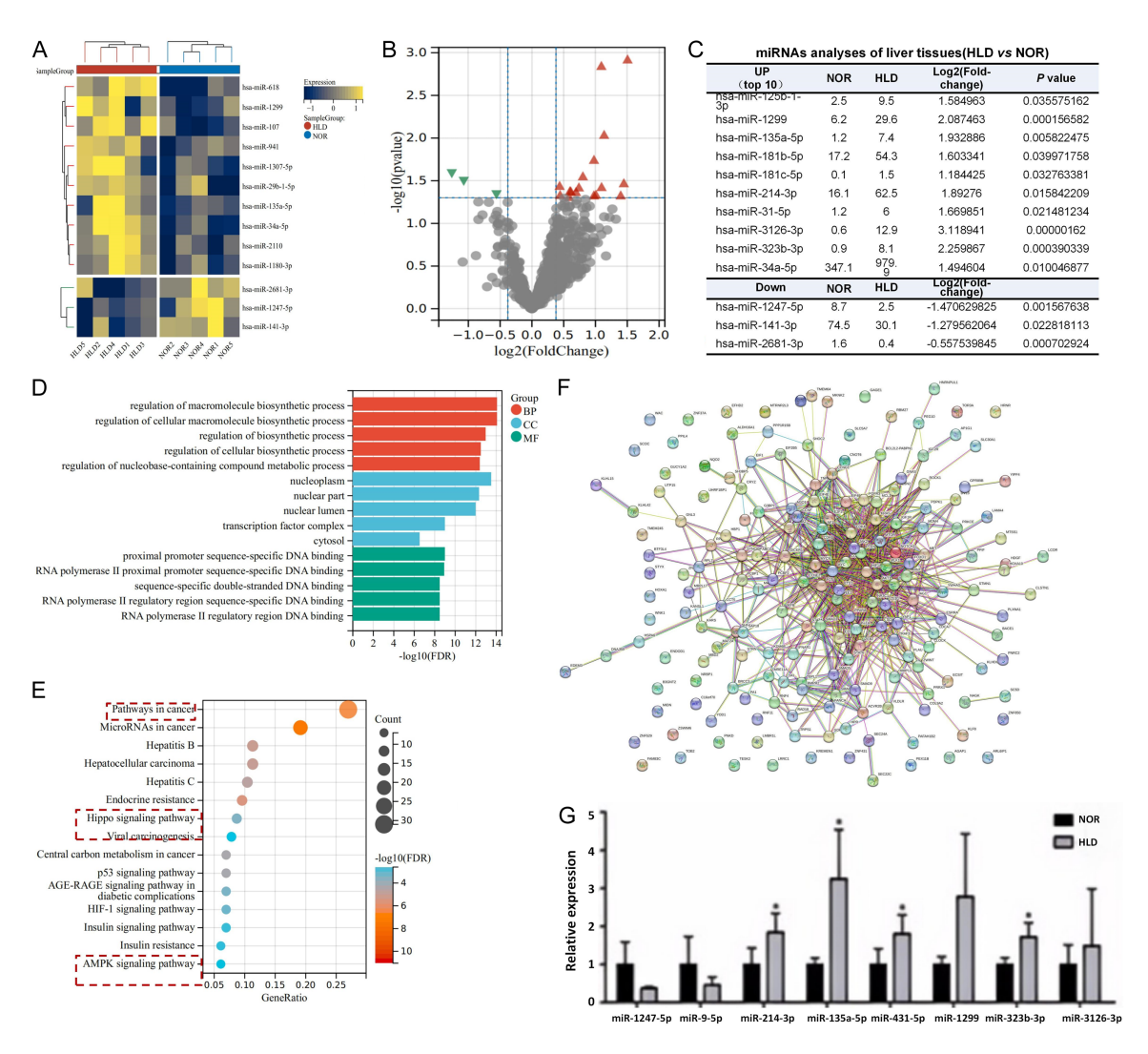
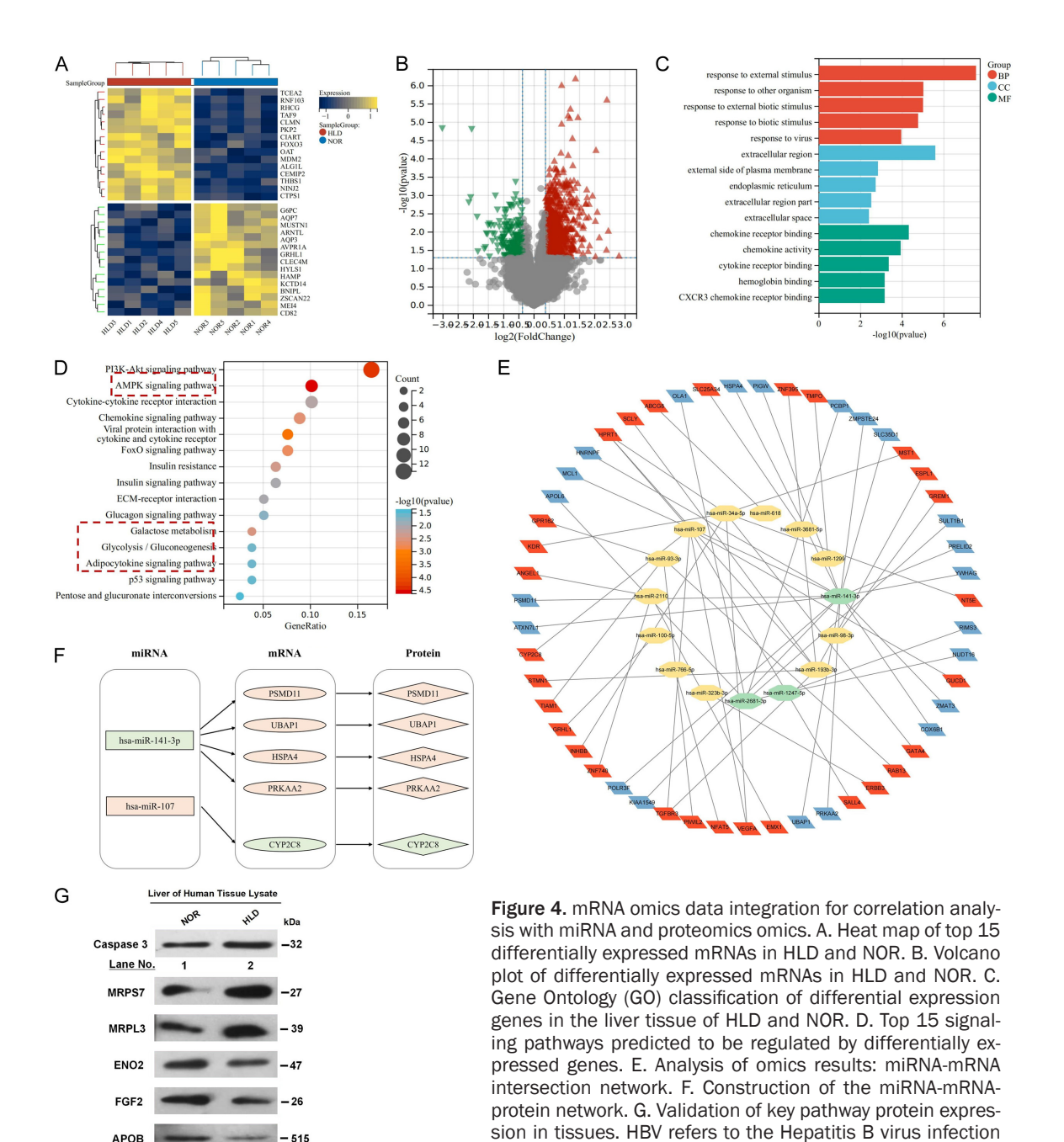


Figure 3. The profiling of miRNAs. A. Heat map of top 15 differentially expressed miRNAs in HLD and NOR. B. Volcano plot of differentially expressed miRNAs in HLD and NOR. C. List of miRNAs with increased and decreased expression in tissues of HLD and NOR patients. D. Gene Ontology (GO) classification of differential expression genes in the liver tissue of HLD and NOR. E. Top 20 signaling pathways predicted to be regulated by differentially expressed genes. F. Protein-Protein Interaction (PPI) network comparison between NOR group and HLD group. NOR, normal group; HLD, hepatolenticular degeneration. G. Validation of differentially expressed miRNAs in tissues.

stain (PAS) staining showed a significant increase in glycogen granule deposition in liver tissue from HLD patients compared to HBV patients (*P < 0.05; Figure 5B). Since HLD is a copper metabolism disorder caused by ATP7B mutation or deletion, we identified R778L as the major mutation site based on ATP7B sequencing of 20 HLD patients, and subsequently constructed ATP7B R778L mutant lentivirus (ATP7B mut) accordingly (Figure 5C). To further investigate how ATP7B mutation or deletion affects tumor metabolism, we overexpressed ATP7B mut in two hepatocellular carcinoma cell lines, MHCC-97H and Huh-7, and

treated the cells with the AMPK pathway activator (metformin) or AMPK pathway inhibitor (compound C) under energy-sufficient or energy-deficient conditions, respectively. As shown in **Figure 5**, overexpression of the ATP7B mut activated the Hippo signaling pathway (*P < 0.05; lane 1 vs lane 2 and 4 in **Figure 5D**, **5E**), resulting in increased level of Yes-associated protein (YAP)/Phosphor-YAP (P-YAP) and transcriptional coactivator with PDZ-binding motif (TAZ)/Phosphor-TAZ (P-TAZ). Although the ATP7B mut led to activation of AMPK phosphorylation in hepatocytes (data not shown), it had a negligible effect on AMPK phosphorylation in



tumor cells (Figure S5). Furthermore, due to metabolic reprogramming in tumor cells, AMPK phosphorylation varied dramatically between different tumor cells (Figure S5A vs S5B). Although the effect of ATP 7B mut on AMPK phosphorylation was not significant in tumor cells, the AMPK inhibitor Compound C still inhibited the activation of the Hippo signaling in MHCC-97H and Huh-7 cells (*P < 0.05; Figure

5D, 5E, lane 4 vs 5). Similarly, the Hippo signaling was further activated by metformin (*P < 0.05; lane 3 vs lane 4 in Figure 5D, 5E). These results suggest that ATP7B mutants, which mimic HLD, induce a specific activation of the Hippo signaling pathway in HCC cells, and that this activation is dependent on the phosphorylation status of the metabolic stress sensor AMPK.

group, while HLD represents hepatolenticular degeneration.

APOB

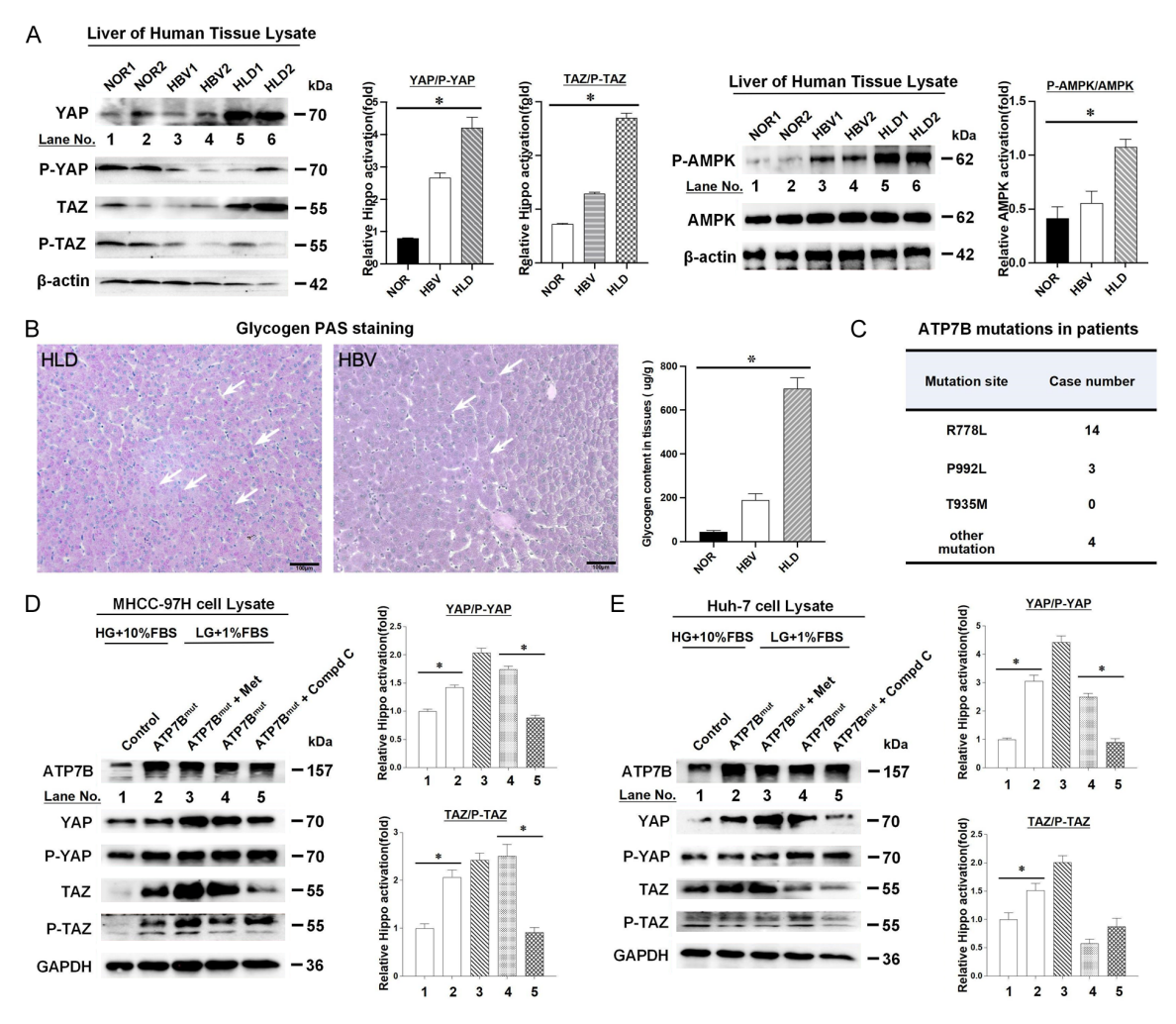


Figure 5. The Hippo and AMPK pathways are activated in HLD patients or overexpression of ATP7B mut . A. Liver tissue samples obtained from individuals with HBV, HLD, or normal conditions were collected and lysed. Hippo and AMPK signaling were assessed with YAP, phospho-YAP (P-YAP), TAZ, and phospho-TAZ (P-TAZ) antibodies. Western blot bands were quantified by densitometry (*P < 0.05, NOR vs HLD). B. Representative images and quantitative analysis of periodic Acid Schiff staining of liver sections (scale bar =100 μ m; *P < 0.05). C. ATP7B mutations identified in HLD patients (n=20). D. MHCC-97H cells, with or without overexpression of ATP7Bmut, were treated with Compound C (10 μ M) or metformin (Met, 1 mM) and cultured under high- or low-glucose conditions. Hippo signaling was assessed with YAP, P-YAP, TAZ, and P-TAZ antibodies. Western blot bands were quantified by densitometry (*P < 0.05). E. Huh-7 cells, with or without overexpression of ATP7Bmut, were treated with Compound C (10 μ M) or metformin (Met, 1 mM) and cultured under high- or low-glucose conditions. Hippo signaling was detected with YAP, P-YAP, TAZ, and P-TAZ antibodies. Western blot bands were quantified by densitometry (*P < 0.05).

Mutation or deletion of ATP7B mimicking HLD inhibits tumor cell progression

Mutation or deletion of the ATP7B gene, mimicking HLD, activates the Hippo signaling pathway, which is often involved in tumor growth and proliferation. However, is unclear how the Hippo signaling activated by mutation or deletion of ATP7B affects the progression of HCC. Two types of hepatocellular carcinoma cells, MHCC-97H and Huh-7, were cultured under

energy-sufficient or energy-deficient conditions. It was found that the proliferative capacity of these cells was significantly higher than that of the ATP7B knockdown cells, suggesting that loss of ATP7B inhibits tumor cell growth (*P < 0.05; **Figure 6A**). MHCC-97H and Huh-7 cells with or without ATP7B knockdown were cultured under low (2% FBS) serum conditions and treated with the Hippo signaling inhibitor Verteporfin or the AMPK signaling inhibitor Compound C (Compd C), respectively. In both

MHCC-97H and Huh-7 cells, the knockdown of ATP7B eliminated the low serum viability of these tumor cells, while the use of Verteporfin could restore this low serum viability to some extent. Whereas the use of Compound C after ATP7B knockdown did not restore the low serum viability of MHCC-97H and Huh-7 cells (*P < 0.05; Figure 6B). Further focus formation assays showed that knockdown of ATP7B significantly restored cell-to-cell contact inhibition in MHCC-97H or Huh-7 cells, thereby inhibiting foci formation (*P < 0.05; Figure 6C, column 1 vs column 2). Verteporfin inhibition of the Hippo pathway caused MHCC-97H and Huh-7 cells to lose cell-cell contact inhibition to some extent (*P < 0.05; Figures 6C and S6A, column 2 vs column 3), partially reserving the malignant transformation of the tumor cells. On the other hand, Compound C also significantly inhibited the formation of foci (*P < 0.05; Figure 6C, column 1 vs column 4), indicating that AMPK phosphorylation is required for the malignant transformation of MHCC-97H and Huh-7 cells. In anchorage-independent growth assays, knockdown of ATP7B significantly inhibited colony formation of MHCC-97H or Huh-7 cells in soft agar (*P < 0.05; Figures 6D and S6B, column 1 vs column 2). Verteporfin, the Hippo signaling inhibitor, caused MHCC-97H and Huh-7 cells to regain the ability to form colonies (*P < 0.05; Figure 6D, column 2 vs column 3). Compound C also significantly inhibited colony formation in soft agar (*P < 0.05; Figure 6D, column 1 vs column 4). In conclusion, mutations or deletions in the ATP7B gene that mimic HLD activate the Hippo signaling pathway and inhibit the proliferation and transformation of HCC cells. This may partly explain why HLD patients exhibit a lower incidence of hepatocellular carcinoma. Figure 6E presents a model demonstrating how ATP7B mutation or deletion in HLD affects the process of liver fibrosis.

Discussion

Liver fibrosis is a natural response to injury and serves as a critical intermediate stage in the progression of most liver diseases. As suggested by the clinical data referenced or presented in this study, fibrosis caused by different factors, such as HBV or HLD, does not differ significantly in physiopathological signs, but does diverge in subsequent disease progression. As the disease progresses, it is clear that HBV-induced fibrosis is more likely to progress to

HCC, the predominant cause of liver cancer. HLD-induced fibrosis, on the other hand, is more likely to progress to liver failure via cirrhosis. HLD is primarily caused by metabolic disorders and is commonly associated with conditions such as obesity, diabetes, and hyperlipidemia. In contrast, liver damage caused by HBV infection is typically the result of chronic inflammation and immune response [42, 43]. These factors may lead to HLD patients experiencing rapid liver failure more easily, while HBV patients undergo a chronic course characterized by inflammation and cellular regeneration, making them more likely to develop HCC [44, 45]. Since HBV and ATP7B mutation/deletion (leading to HLD) are two clear precursors of fibrosis, they are ideal models to study fibrosis, in particular the factors and molecular mechanisms that determine the subsequent disease progression. This study primarily aims to examine these aspects. As the largest metabolic organ in the human body, alterations in liver metabolism undoubtedly play a central role in most liver diseases. Hence, our research focused on the changes in metabolic orchestration resulting from HBV infection or ATP7B mutation/deletion, differences in specific molecules and pathways, and how these variations influence tumor progression.

In the present study, we first confirmed in a retrospective clinical study that liver disease progression of liver disease follows different pathways after the induction of liver fibrosis by either HBV or HLD. We then used proteomics, RNA-seg and combined analyses of clinical samples to identify differences in specific molecules and signaling pathways in HBV- or HLDinduced liver fibrosis. In subsequent studies, we focused on the effects of metabolic stress, represented by AMPK phosphorylation and Hippo pathway activation, on HCC progression. We validated the inhibitory effect of the Hippo pathway on HCC progression in response to metabolic changes caused by ATP7B mutation/ deletion. Our findings elucidate the relationship between differences in metabolic stresses and alterations, activation of the Hippo pathway and the direction of subsequent disease progression in liver fibrosis from different causes. At present, we only know that metabolic changes, such as metabolic stress signaled by AMPK, can influence the activation of the Hippo signaling, but the exact mechanism remains unclear and requires further investigation. There is a

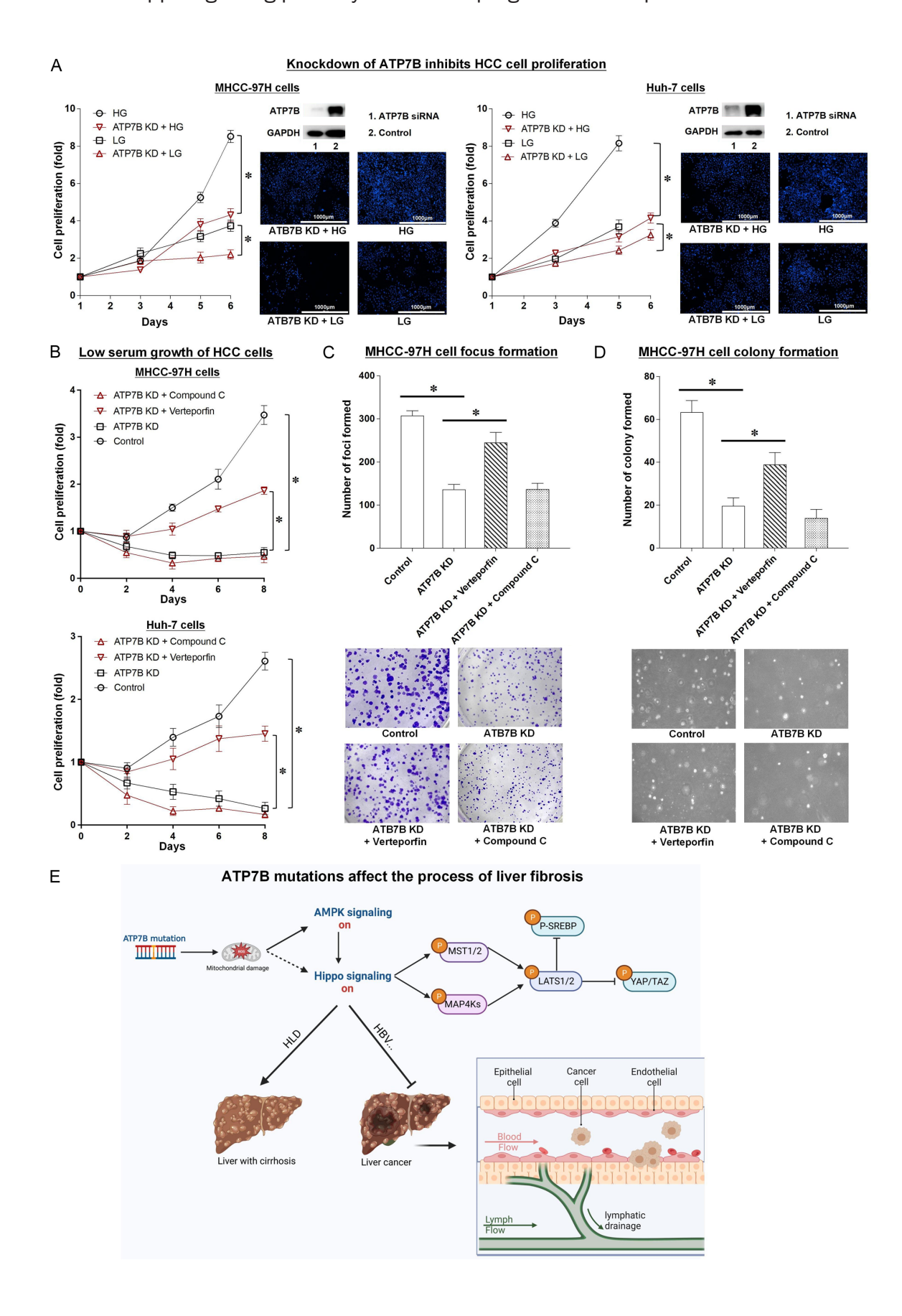


Figure 6. Knockdown of ATP7B inhibit the proliferation of HCC cells. A. Left graph: Proliferation (number of cells increased (folds) at different time points) of MHCC-97H cells with or without ATP7B knockdown, cultured under high or low glucose conditions. Right graph: Proliferation (number of cells increased (folds) at different time points) of Huh-7 cells with or without ATP7B knockdown, cultured under high or low glucose conditions. HG: 4.5 g/L Glucose; LG: 1 g/L Glucose (scale bar =1000 μ m; *P < 0.05). B. Top graph: MHCC-97H cell proliferation (the number of cells increased (folds) at different time points): MHCC-97H cells without or with ATP7B knockdown, treated without or with Hippo (Verteporfin, 3 μM) or AMPK (Compound C, 10 μM) signaling pathway inhibitors, were cultured under low serum (2% FBS) conditions (*P < 0.05). Bottom graph: Huh-7 cell proliferation (the number of cells increased (folds) at different time points): Huh-7 cells without or with ATP7B knockdown, treated without or with Verteporfin (3 μ M) or Compound C (10 μ M), were cultured under low serum (2% FBS) conditions (*P < 0.05). C. MHCC-97H cell focus formation assay: MHCC-97H cells without or with ATP7B knockdown were treated without or with Verteporfin (3 μM) or Compound C (10 μM). The number of foci formed was counted (*P < 0.05). D. MHCC-97H cell colony formation assay: MHCC-97H cells without or with ATP7B knockdown were treated without or with Verteporfin (3 µM) or Compound C (10 µM). The number of colony formed in soft agar was counted (*P < 0.05). E. Schematic illustration of the mechanism: Mutations in the ATP7B modulate the expression of AMPK and Hippo signaling pathway-related proteins, thereby influencing the progression of hepatic fibrosis and altering the final disease outcome.

consensus in the research community that the Hippo signaling pathway is closely linked to tumor progression. A large number of studies have shown that its activated state promotes tumor size, growth and proliferation, and it is also closely linked to glycolipid metabolism. Its downstream SREBP2 is a transcription factor and a primary regulator of cholesterol homeostasis [46-49]. Studies have also found that the phosphorylation of AMPK or the activation of the Hippo signaling pathway can also inhibit the progression of liver fibrosis [50]. This may partly explain why HLD patients are less likely to progress to HCC [51]. Unexpectedly, we found that activation of the Hippo pathway by ATP7B mutation had an anti-tumor effect, highlighting the dual nature of the Hippo pathway in tumor progression. In our study, we also found that ATP7B mutation led to glycogen accumulation and increased ROS. The relevance of these changes to tumor progression needs to be further investigated.

HLD is a disease characterized by abnormal copper metabolism caused by mutation or deletion in ATP7B, which is usually characterized by abnormal copper homeostasis and copper overload, particularly in the liver. Given that clinical patients usually undergo copper detoxification treatments and that we did not include copper ions in our cellular experiments, this suggests that the effect of ATP7B mutation on tumor progression in our subsequent experiments was independent of copper toxicity, a point we would like to clarify here.

In conclusion, our findings partially elucidate the mechanism by which different causes of liver fibrosis take different directions in subsequent disease progression. The discovery of the key role of the Hippo pathway here provides new approaches and ideas for potential treatment, as well as new avenues for exploring the relationship between the Hippo pathway and cancer progression.

Acknowledgements

We acknowledge members of the Qiyu laboratory, members of the institute of Chinese Medicine Surgery, and Peng Zhai from Boston University for critically reading the manuscript. We acknowledge the support from Cancer Research Center, The First Affiliated Hospital of USTC, Division of Life Sciences and Medicine, University of Science and Technology of China. Figures 1A and 6E were modified from: https:// app.biorender.com (Permission obtained). This work was supported by grants from National Natural Science foundation of China (NSFC: 81773112 and 82073186 for Q.F.). This work was supported by Construction project of the State Administration of Traditional Chinese Medicine in 2021 (Teaching Letter [2021] No. 270 for Q.Y) and Anhui Province Clinical Key Specialty Project in 2022 (Anhui Weichuan [2022] No. 297 for Q.Y).

Informed consent had been obtained from all participants.

Disclosure of conflict of interest

None.

Address correspondence to: Qingsheng Yu and Hui Peng, Department of General Surgery, The First Affiliated Hospital of Anhui University of Chinese Medicine, Hefei 230031, Anhui, P. R. China. Tel:

+86-13866141906; E-mail: qsy6312@163.com (QSY); Tel: +86-15955916472; E-mail: ph13638-2333@126.com (HP); Qiyu Feng, Cancer Research Center, The First Affiliated Hospital of USTC, Division of Life Sciences and Medicine, University of Science and Technology of China, Hefei 230036, Anhui, P. R. China. Tel: +86-0551-63607040; E-mail: qiyufeng@ustc.edu.cn

References

- [1] Kisseleva T and Brenner D. Molecular and cellular mechanisms of liver fibrosis and its regression. Nat Rev Gastroenterol Hepatol 2021; 18: 151-166.
- [2] Parola M and Pinzani M. Liver fibrosis: pathophysiology, pathogenetic targets and clinical issues. Mol Aspects Med 2019; 65: 37-55.
- [3] Kotsiliti E. Lactylation and HCC progression. Nat Rev Gastroenterol Hepatol 2023; 20: 131.
- [4] Karsdal MA, Daniels SJ, Holm Nielsen S, Bager C, Rasmussen DGK, Loomba R, Surabattula R, Villesen IF, Luo Y, Shevell D, Gudmann NS, Nielsen MJ, George J, Christian R, Leeming DJ and Schuppan D. Collagen biology and non-invasive biomarkers of liver fibrosis. Liver Int 2020; 40: 736-750.
- [5] Berumen J, Baglieri J, Kisseleva T and Mekeel K. Liver fibrosis: pathophysiology and clinical implications. WIREs Mech Dis 2021; 13: e1499.
- [6] Rashid A, Gupta A, Adiamah A, West J, Grainge M and Humes DJ. Mortality following appendicectomy in patients with liver cirrhosis: a systematic review and meta-analysis. World J Surg 2022; 46: 531-541.
- [7] Roehlen N, Crouchet E and Baumert TF. Liver fibrosis: mechanistic concepts and therapeutic perspectives. Cells 2020; 9: 875.
- [8] Friedman SL and Pinzani M. Hepatic fibrosis 2022: unmet needs and a blueprint for the future. Hepatology 2022; 75: 473-488.
- [9] Liang C, Liu J, Jiang M, Zhu Y and Dong P. The advancement of targeted regulation of hepatic stellate cells using traditional Chinese medicine for the treatment of liver fibrosis. J Ethnopharmacol 2025; 341: 119298.
- [10] Shree Harini K and Ezhilarasan D. Wnt/betacatenin signaling and its modulators in nonalcoholic fatty liver diseases. Hepatobiliary Pancreat Dis Int 2023; 22: 333-345.
- [11] Yadav P, Singh SK, Rajput S, Allawadhi P, Khurana A, Weiskirchen R and Navik U. Therapeutic potential of stem cells in regeneration of liver in chronic liver diseases: current perspectives and future challenges. Pharmacol Ther 2024; 253: 108563.
- [12] Bresciani N, Demagny H, Lemos V, Pontanari F, Li X, Sun Y, Li H, Perino A, Auwerx J and

- Schoonjans K. The Slc25a47 locus is a novel determinant of hepatic mitochondrial function implicated in liver fibrosis. J Hepatol 2022; 77: 1071-1082.
- [13] Xu L, Yang TY, Zhou YW, Wu MF, Shen J, Cheng JL, Liu QX, Cao SY, Wang JQ and Zhang L. Bmal1 inhibits phenotypic transformation of hepatic stellate cells in liver fibrosis via IDH1/alpha-KG-mediated glycolysis. Acta Pharmacol Sin 2022; 43: 316-329.
- [14] Pope ED 3rd, Kimbrough EO, Vemireddy LP, Surapaneni PK, Copland JA 3rd and Mody K. Aberrant lipid metabolism as a therapeutic target in liver cancer. Expert Opin Ther Targets 2019; 23: 473-483.
- [15] Xu K, Xia P, Chen X, Ma W and Yuan Y. ncRNAmediated fatty acid metabolism reprogramming in HCC. Trends Endocrinol Metab 2023; 34: 278-291.
- [16] Dai W, Xu L, Yu X, Zhang G, Guo H, Liu H, Song G, Weng S, Dong L, Zhu J, Liu T, Guo C and Shen X. OGDHL silencing promotes hepatocellular carcinoma by reprogramming glutamine metabolism. J Hepatol 2020; 72: 909-923.
- [17] Kar A, Samanta A, Mukherjee S, Barik S and Biswas A. The HBV web: an insight into molecular interactomes between the hepatitis B virus and its host en route to hepatocellular carcinoma. J Med Virol 2023; 95: e28436.
- [18] Tu T, McQuaid TJ and Jacobson IM. HBV-induced carcinogenesis: mechanisms, correlation with viral suppression, and implications for treatment. Liver Int 2025; 45: e16202.
- [19] Cho HJ and Cheong JY. Role of immune cells in patients with hepatitis B virus-related hepatocellular carcinoma. Int J Mol Sci 2021; 22: 8011.
- [20] Lin YT, Jeng LB, Chan WL, Su IJ and Teng CF. Hepatitis B virus Pre-S gene deletions and Pre-S deleted proteins: clinical and molecular implications in hepatocellular carcinoma. Viruses 2021; 13: 862.
- [21] Piracha ZZ, Saeed U, Piracha IE, Noor S and Noor E. Decoding the multifaceted interventions between human sirtuin 2 and dynamic hepatitis B viral proteins to confirm their roles in HBV replication. Front Cell Infect Microbiol 2023; 13: 1234903.
- [22] Toh MR, Wong EYT, Wong SH, Ng AWT, Loo LH, Chow PK and Ngeow J. Global epidemiology and genetics of hepatocellular carcinoma. Gastroenterology 2023; 164: 766-782.
- [23] Singal AG, Kanwal F and Llovet JM. Global trends in hepatocellular carcinoma epidemiology: implications for screening, prevention and therapy. Nat Rev Clin Oncol 2023; 20: 864-884.
- [24] Schilsky ML, Czlonkowska A, Zuin M, Cassiman D, Twardowschy C, Poujois A, Gondim FAA,

- Denk G, Cury RG, Ott P, Moore J, Ala A, D'Inca R, Couchonnal-Bedoya E, D'Hollander K, Dubois N, Kamlin COF and Weiss KH; CHELATE trial investigators. Trientine tetrahydrochloride versus penicillamine for maintenance therapy in Wilson disease (CHELATE): a randomised, open-label, non-inferiority, phase 3 trial. Lancet Gastroenterol Hepatol 2022; 7: 1092-1102.
- [25] Czlonkowska A, Litwin T, Dusek P, Ferenci P, Lutsenko S, Medici V, Rybakowski JK, Weiss KH and Schilsky ML. Wilson disease. Nat Rev Dis Primers 2018; 4: 21.
- [26] Polishchuk EV, Merolla A, Lichtmannegger J, Romano A, Indrieri A, Ilyechova EY, Concilli M, De Cegli R, Crispino R, Mariniello M, Petruzzelli R, Ranucci G, Iorio R, Pietrocola F, Einer C, Borchard S, Zibert A, Schmidt HH, Di Schiavi E, Puchkova LV, Franco B, Kroemer G, Zischka H and Polishchuk RS. Activation of autophagy, observed in liver tissues from patients with Wilson disease and from ATP7B-deficient animals, protects hepatocytes from copper-induced apoptosis. Gastroenterology 2019; 156: 1173-1189, e1175.
- [27] Haber PS, Riordan BC, Winter DT, Barrett L, Saunders J, Hides L, Gullo M, Manning V, Day CA, Bonomo Y, Burns L, Assan R, Curry K, Mooney-Somers J, Demirkol A, Monds L, McDonough M, Baillie AJ, Clark P, Ritter A, Quinn C, Cunningham J, Lintzeris N, Rombouts S, Savic M, Norman A, Reid S, Hutchinson D, Zheng C, Iese Y, Black N, Draper B, Ridley N, Gowing L, Stapinski L, Taye B, Lancaster K, Stjepanovic D, Kay-Lambkin F, Jamshidi N, Lubman D, Pastor A, White N, Wilson S, Jaworski AL, Memedovic S, Logge W, Mills K, Seear K, Freeburn B, Lea T, Withall A, Marel C, Boffa J, Roxburgh A, Purcell-Khodr G, Doyle M, Conigrave K, Teesson M, Butler K, Connor J and Morley KC. New Australian guidelines for the treatment of alcohol problems: an overview of recommendations. Med J Aust 2021; 215 Suppl 7: S3-S32.
- [28] Diao Y, Tang J, Wang X, Deng W, Tang J and You C. Metabolic syndrome, nonalcoholic fatty liver disease, and chronic hepatitis B: a narrative review. Infect Dis Ther 2023; 12: 53-66.
- [29] Liu SQ, Yang YP, Hussain N, Jian YQ, Li B, Qiu YX, Yu HH, Wang HZ and Wang W. Dibenzocy-clooctadiene lignans from the family schisand-raceae: a review of phytochemistry, structure-activity relationship, and hepatoprotective effects. Pharmacol Res 2023; 195: 106872.
- [30] Horn P and Tacke F. Metabolic reprogramming in liver fibrosis. Cell Metab 2024; 36: 1439-1455.
- [31] Mohseni R, Teimouri M, Safaei M and Arab Sadeghabadi Z. AMP-activated protein kinase

- is a key regulator of obesity-associated factors. Cell Biochem Funct 2023; 41: 20-32.
- [32] Entezari M, Hashemi D, Taheriazam A, Zabolian A, Mohammadi S, Fakhri F, Hashemi M, Hushmandi K, Ashrafizadeh M, Zarrabi A, Ertas YN, Mirzaei S and Samarghandian S. AMPK signaling in diabetes mellitus, insulin resistance and diabetic complications: a pre-clinical and clinical investigation. Biomed Pharmacother 2022; 146: 112563.
- [33] Iorio R, Celenza G and Petricca S. Mitophagy: molecular mechanisms, new concepts on parkin activation and the emerging role of AMPK/ ULK1 axis. Cells 2021; 11: 30.
- [34] Xue Q, Kang R, Klionsky DJ, Tang D, Liu J and Chen X. Copper metabolism in cell death and autophagy. Autophagy 2023; 19: 2175-2195.
- [35] Chen Y and Tian Z. HBV-induced immune imbalance in the development of HCC. Front Immunol 2019; 10: 2048.
- [36] Russell JO and Camargo FD. Hippo signalling in the liver: role in development, regeneration and disease. Nat Rev Gastroenterol Hepatol 2022; 19: 297-312.
- [37] Kim W, Khan SK, Liu Y, Xu R, Park O, He Y, Cha B, Gao B and Yang Y. Hepatic Hippo signaling inhibits protumoural microenvironment to suppress hepatocellular carcinoma. Gut 2018; 67: 1692-1703.
- [38] Fulco M, Cen Y, Zhao P, Hoffman EP, McBurney MW, Sauve AA and Sartorelli V. Glucose restriction inhibits skeletal myoblast differentiation by activating SIRT1 through AMPK-mediated regulation of Nampt. Dev Cell 2008; 14: 661-673.
- [39] Jeon SM, Chandel NS and Hay N. AMPK regulates NADPH homeostasis to promote tumour cell survival during energy stress. Nature 2012; 485: 661-665.
- [40] Liang J and Mills GB. AMPK: a contextual oncogene or tumor suppressor? Cancer Res 2013; 73: 2929-2935.
- [41] Bungard D, Fuerth BJ, Zeng PY, Faubert B, Maas NL, Viollet B, Carling D, Thompson CB, Jones RG and Berger SL. Signaling kinase AMPK activates stress-promoted transcription via histone H2B phosphorylation. Science 2010; 329: 1201-1205.
- [42] Llovet JM, Willoughby CE, Singal AG, Greten TF, Heikenwälder M, El-Serag HB, Finn RS and Friedman SL. Nonalcoholic steatohepatitis-related hepatocellular carcinoma: pathogenesis and treatment. Nat Rev Gastroenterol Hepatol 2023; 20: 487-503.
- [43] Lin X, Zhang J, Chu Y, Nie Q and Zhang J. Berberine prevents NAFLD and HCC by modulating metabolic disorders. Pharmacol Ther 2024; 254: 108593.

Hippo signaling pathway affects the progression of hepatocarcinoma

- [44] Nakamura T, Masuda A, Nakano D, Amano K, Sano T, Nakano M and Kawaguchi T. Pathogenic Mechanisms of Metabolic Dysfunction-Associated Steatotic Liver Disease (MASLD)associated hepatocellular carcinoma. Cells 2025; 14: 428.
- [45] Xie D, Shi J, Zhou J, Fan J and Gao Q. Clinical practice guidelines and real-life practice in hepatocellular carcinoma: a Chinese perspective. Clin Mol Hepatol 2023; 29: 206-216.
- [46] Sorrentino G, Ruggeri N, Specchia V, Cordenonsi M, Mano M, Dupont S, Manfrin A, Ingallina E, Sommaggio R, Piazza S, Rosato A, Piccolo S and Del Sal G. Metabolic control of YAP and TAZ by the mevalonate pathway. Nat Cell Biol 2014; 16: 357-366.
- [47] Wang Y, Yang H, Su X, Cao A, Chen F, Chen P, Yan F and Hu H. SREBP2 promotes the viability, proliferation, and migration and inhibits apoptosis in TGF-beta1-induced airway smooth muscle cells by regulating TLR2/NF-kappaB/ NFATc1/ABCA1 regulatory network. Bioengineered 2022; 13: 3137-3147.

- [48] Zhao B, Li L, Tumaneng K, Wang CY and Guan KL. A coordinated phosphorylation by Lats and CK1 regulates YAP stability through SCF (beta-TRCP). Genes Dev 2010; 24: 72-85.
- [49] Li F, Wang Y, Zeller KI, Potter JJ, Wonsey DR, O'Donnell KA, Kim JW, Yustein JT, Lee LA and Dang CV. Myc stimulates nuclearly encoded mitochondrial genes and mitochondrial biogenesis. Mol Cell Biol 2005; 25: 6225-6234.
- [50] Lv T, Fan X, He C, Zhu S, Xiong X, Yan W, Liu M, Xu H, Shi R and He Q. SLC7A11-ROS/αKG-AMPK axis regulates liver inflammation through mitophagy and impairs liver fibrosis and NASH progression. Redox Biology 2024; 72: 103159.
- [51] Pei Q, Yi Q and Tang L. Liver fibrosis resolution: from molecular mechanisms to therapeutic opportunities. Int J Mol Sci 2023; 24: 9671.

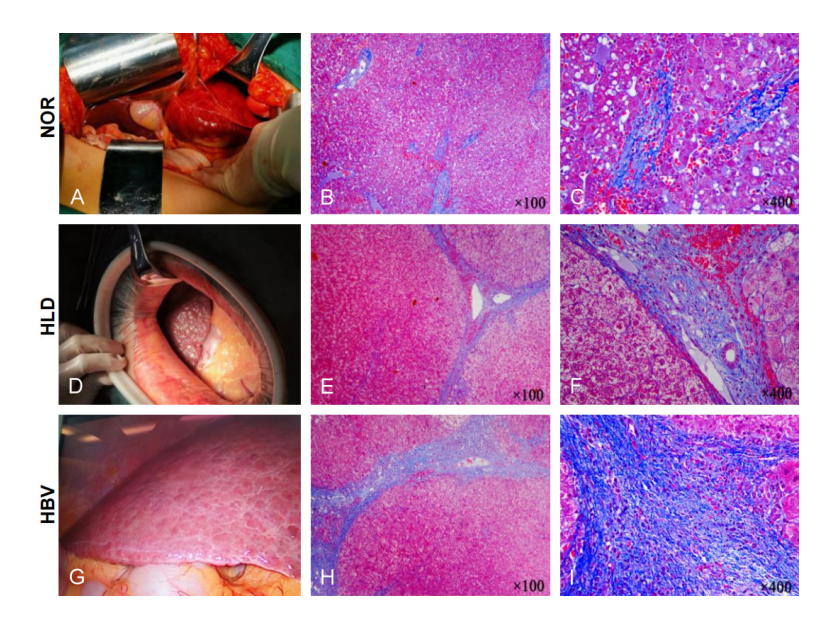


Figure S1. Masson's staining of the patient's liver tissue. A. The normal liver tissue of the patient with hepatic haemangioma. B and C. Masson's staining of normal liver tissue under 100× and 400× microscope. D. Liver tissue from a patient with HLD. E and F. Masson's stain of HLD liver tissue under 100× and 400× microscope. G. Liver tissue from HBV patients. H and I. Masson's stain of HBV liver tissue under 100× and 400× microscope.

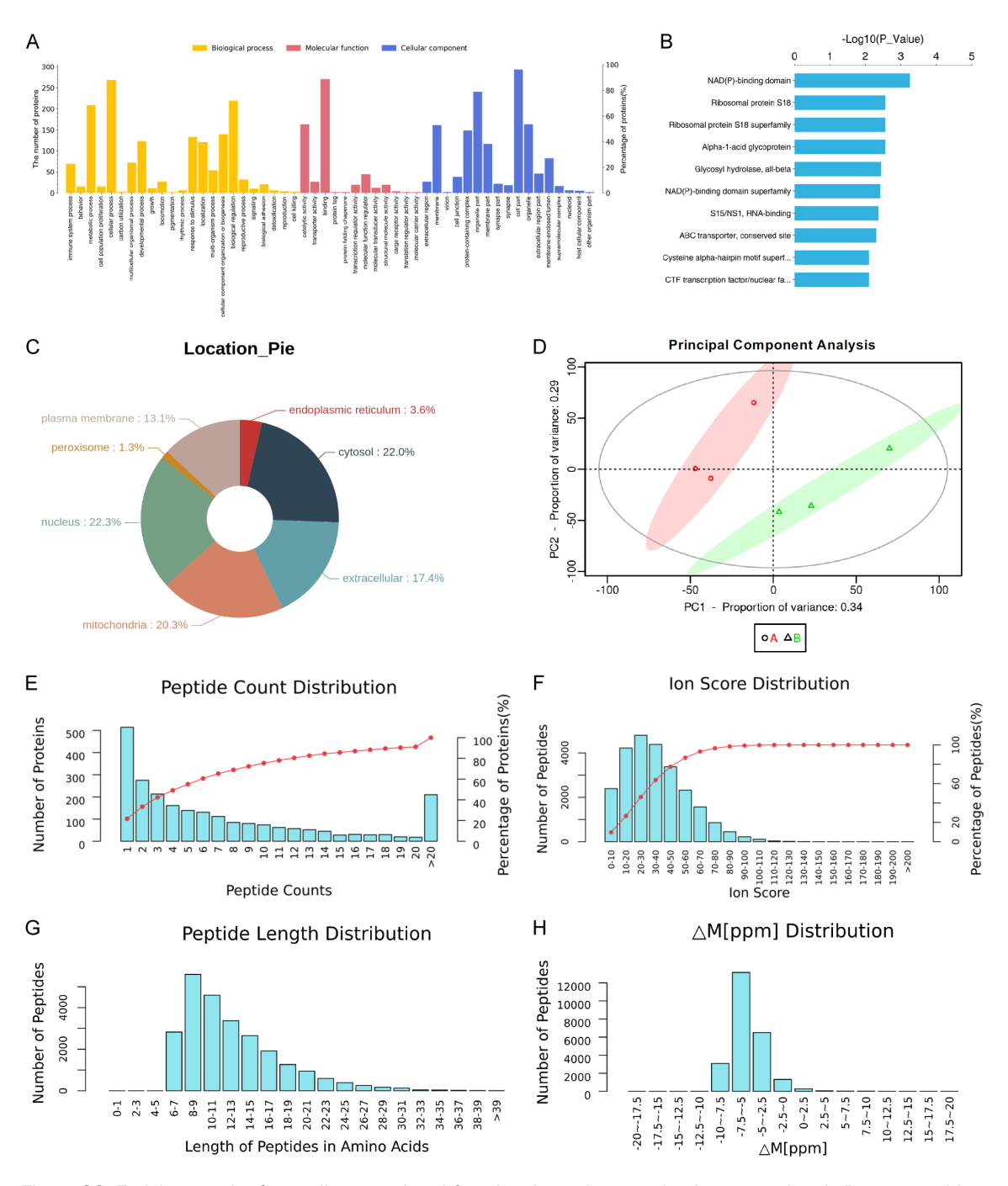


Figure S2. Enrichment plot for quality control and functional supplementation in proteomics. A. Percentage histogram of GO functions. B. Percentage histogram of KEGG enrichment. C. Location Pie of Proteomics. D. Principal Component Analysis of Proteomics. E. Distribution of Identified Peptide Counts in Proteomics. F. Distribution of Peptide Ion Scores. G. Distribution of Peptide Sequence Lengths. H. Distribution of Peptide Mass Deviations.

Hippo signaling pathway affects the progression of hepatocarcinoma

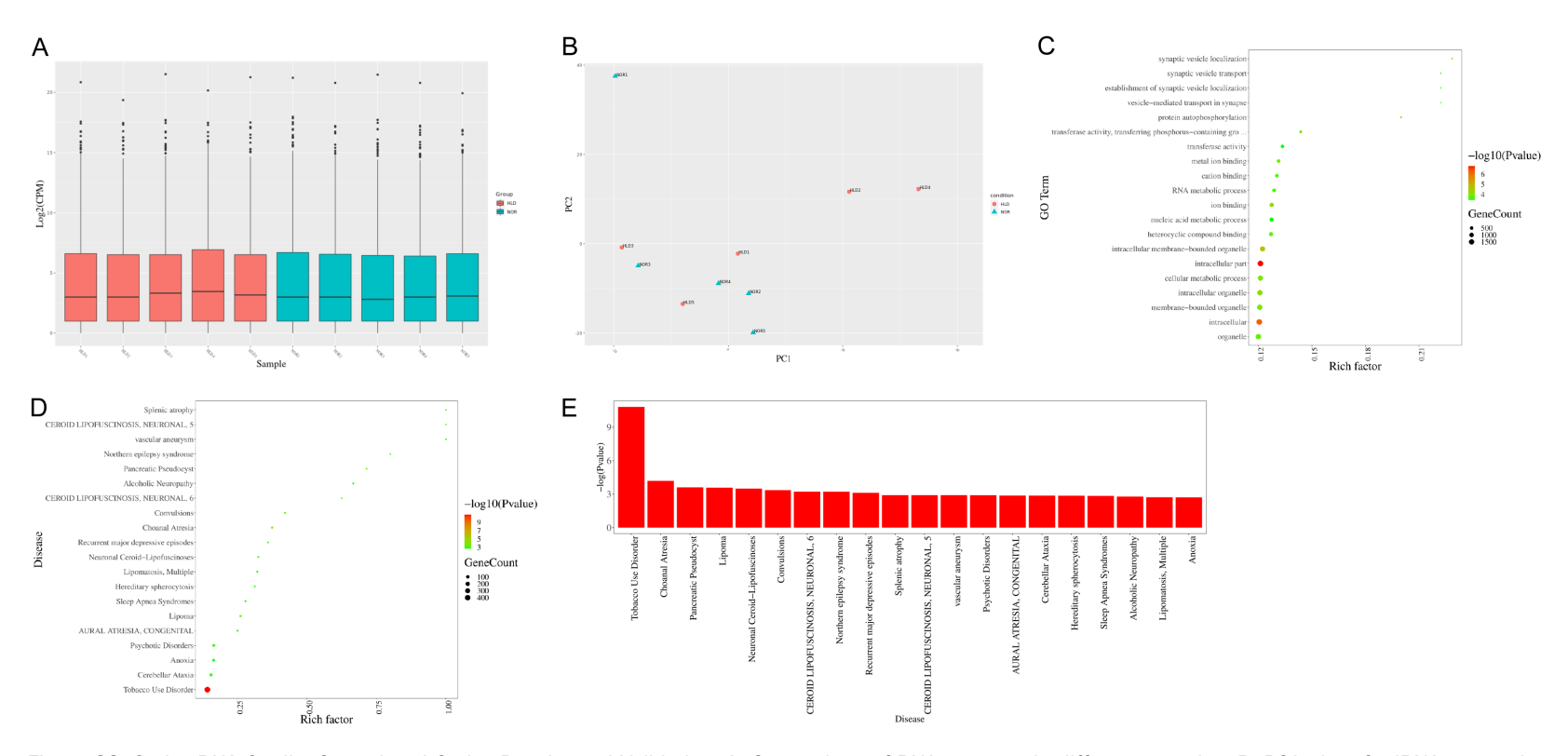


Figure S3. Omics RNA Quality Control and Omics Results and Validation. A. Comparison of RNA contents in different samples. B. PCA plot of miRNA expression abundance. C. Significant Enrichment GO Scatterplot. D. Disease Enrichment Dot Plot. E. Disease Enrichment Bar Plot.

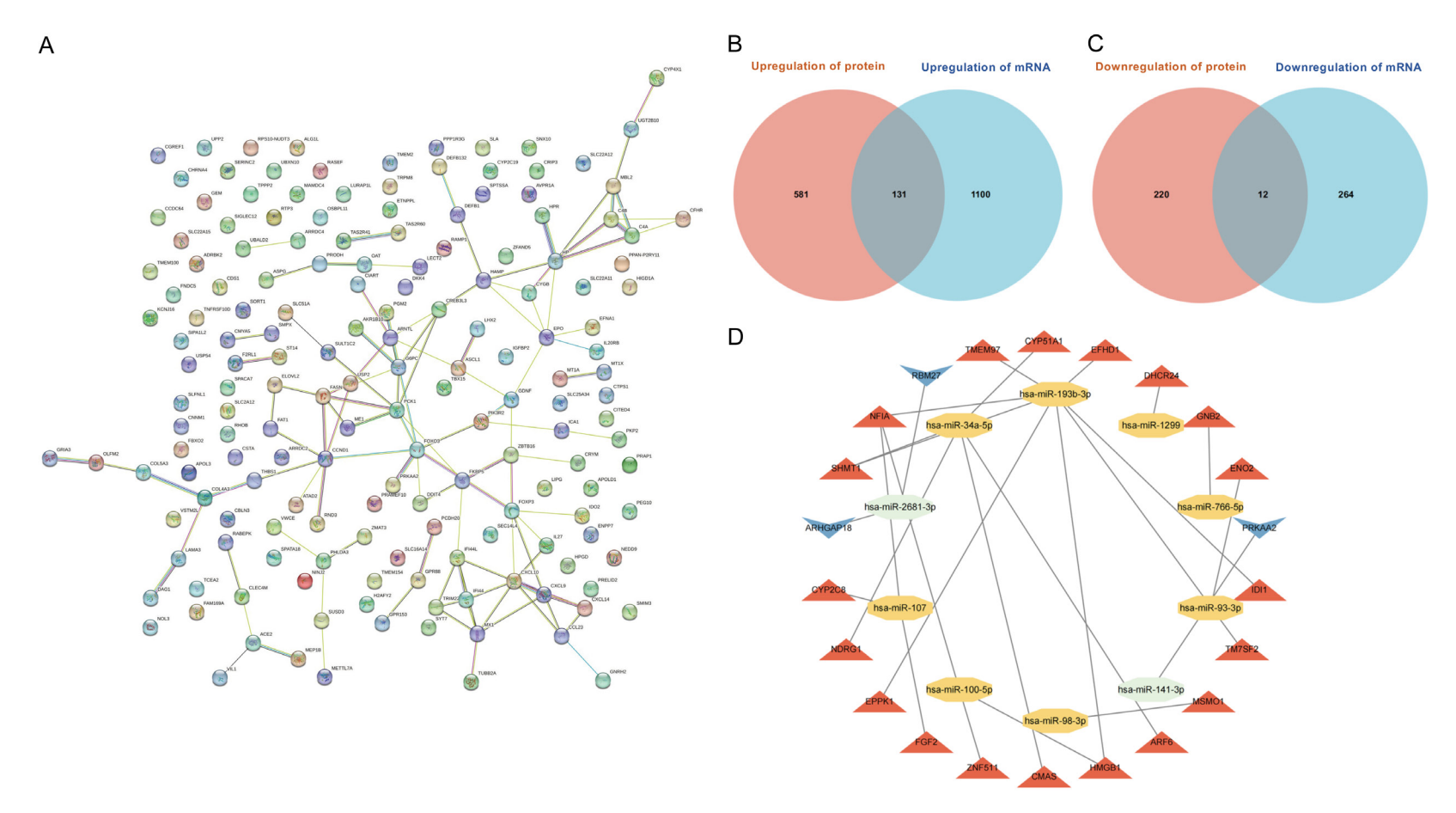


Figure S4. Multi-omics integrative analysis. A. Network of differentially expressed mRNAs. B. Intersection of Upregulated Expression in Proteomics and mRNA omics. C. Intersection of Downregulated Expression in Proteomics and mRNA omics. D. miRNA and Protein Interaction Network.

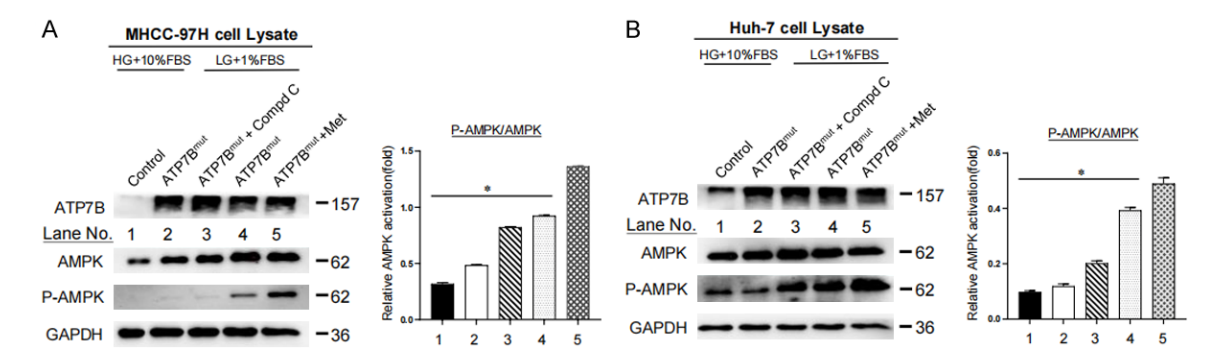


Figure S5. The AMPK pathways are activated after overexpression of ATP7B mut . A. MHCC-97H cells without or with overexpression of ATP7B mut , treated without or with Compound C or metformin, were cultured under high- or low-glucose culture conditions. AMPK signaling was detected using AMPK and phospho-AMPK (P-AMPK) antibodies. Western blot bands were quantified by densitometry (*P < 0.05). B. Huh-7 cells without or with overexpression of ATP7B mut , treated without or with Compound C or metformin, were cultured under high- or low-glucose culture conditions. AMPK signaling was detected using AMPK and phospho-AMPK (P-AMPK) antibodies. Western blot bands were quantified by densitometry (*P < 0.05).

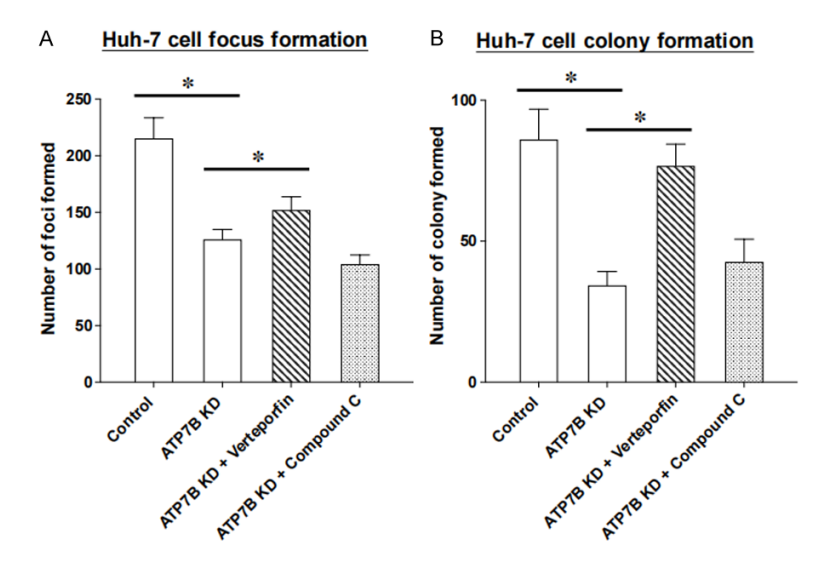


Figure S6. Knockdown of ATP7B inhibits HCC cell proliferation. A. Huh-7 cell focus formation assay: Huh-7 cells without or with ATP7B knockdown were treated without or with Verteporfin or Compound C. The number of foci formed was counted ($^{*}P < 0.05$). B. Huh-7 cell colony formation assay: Huh-7 cells without or with ATP7B knockdown were treated without or with Verteporfin or Compound C. The number of colonies formed in soft agar was counted ($^{*}P < 0.05$). The number of colony formed in soft agar was counted ($^{*}P < 0.05$).